A novel image registration method for InISAR 3D imaging

Zibo Zhou[1,a], Libing Jiang[1] and Zhuang Wang[1]

[1]*College of Electronic Science, National University of Defense Technology, 410073 Changsha, China.*

Abstract. Image registration is a key intermediate step for Interferometric Inverse Synthetic Aperture Radar (InISAR) three-dimensional (3D) imaging. It arranges the same scatterers of the target on the same pixel cell in different ISAR images, which makes the interferometric processing carried on between the same scatterers to obtain its 3D coordinates. This paper proposes a novel ISAR image registration method of three steps. Firstly, chirp Fourier transform is used to estimate the rotational angular velocity of the target. Secondly, the compensation phase is constructed, according to the rotational angular velocity, to eliminate the wave path difference between different radars echoes. Finally, two-dimensional (2D) Fourier transform is used to yield registered ISAR images. The proposed method achieves the ISAR image registration through phase compensation in echo field, therefore, no extra computation is needed in image field. The experiment results demonstrate the advantages of the proposed method in precision, computation efficiency and practicability.

1 Introduction

Radar imaging is a hot subject in radar signal processing. With the higher requirements for target recognition and the development of modern wideband high-resolution radar, Interferometric Inverse Synthetic Aperture Radar (InISAR) 3D imaging has gradually become a hot issue in the field of radar imaging [1-4].

During the InISAR 3D imaging processing, ISAR image registration is a key intermediate step, whose purpose is to arrange the same scatterers of the target on the same pixel cell in different images and ensure that the interferometric process is performed between the same scatterers. Since the interferometric phase difference contains the coordinate information of the scatterers, the 3D structure of the target can be obtained [5].

There are many literatures and applications concerning ISAR image registration and InISAR 3D imaging techniques. The correlation coefficient based image registration method, which was widely used for SAR image registration, was firstly introduced to solve the ISAR image registration problem [6,7]. Wang et al. [8] presented a SAR image registration method based on integrating real and complex correlation function. Through coregistration sensitive factor, the appropriate correlation function is selected to measure the quality of image registration. However, the targets observed by SAR and ISAR are different. And the target of ISAR only account for a small part of the ISAR image, so the correlation coefficient is easily affected by noise. Zhang et al. [9] proposed a multi-antenna configuration InISAR imaging system, which arranges multiple antennas along two vertical baseline directions. The antennas on the larger baseline are used to estimate the rotational angle, while the antennas on the smaller baseline are used for ISAR imaging. By using the wave path difference calculated by the rotational angle to compensate the echoes, the mismatch between the ISAR images is eliminated. However, the five-antenna imaging system increases the cost of hardware.

Aiming at the high precision and low hardware cost, this paper proposes a novel image registration method based on wave path difference compensation. Firstly, the chirp Fourier transform is used to estimate the rotational angular velocity of the target relative to the radar. Then the wave path compensation phase is constructed and the echo is compensated to eliminate the mismatch between ISAR images.

The rest of this paper is organized as follows: Section II analyses the L-shaped three-antenna InISAR 3D image model. Section III is devoted to the ISAR image registration method based on wave path difference compensation. Section IV introduces the simulation experiment result. Finally, Section V draws conclusion on the proposed imaging method.

2 L-shaped InISAR 3D image model

The geometric configuration of the L-shaped three-antenna InISAR imaging system is shown in Figure 1, which contains two orthogonal coordinate systems in parallel, i.e., the radar coordinate system (A-XYZ) and the target coordinate system (O-xyz). The locations of three radars in radar coordinate system are $A(0,0,0)$, $B(0,0,L)$ and $C(L,0,0)$ respectively. Only radar A

[a] Corresponding author: zibo_travel@163.com

transmits electromagnetic wave and all the three radars receive echo pulses from the target. The baselines AB and AC are perpendicular to each other and they have the same length, denoted as *L*. The origin (i.e., reference point) of the target coordinate system is located at the geometric centre of the target at position $O(X_0, Y_0, Z_0)$ in the radar coordinate system. $\hat{t}$ is the imaging fast-time, and t_m is the imaging slow-time. The distance from *O* to radar A, B, and C is R_{OA}, R_{OB} and R_{OC}, respectively, which are functions of slow-time t_m. *P* is the *k*th scatterer on the target, which position in target coordinate system is (x_k, y_k, z_k). The distance from *P* to radar A, B, and C is R_{Ak}, R_{Bk} and R_{Ck} respectively. And the motion velocity of the target along $\overline{AO}$, $\overline{BO}$ and $\overline{CO}$ directions is V_{Ak}, V_{Bk} and V_{Ck}, respectively.

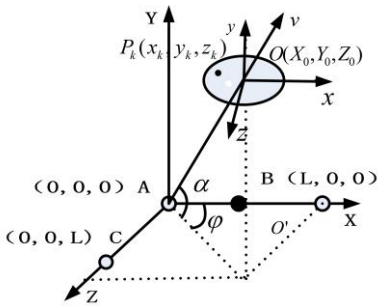

Figure 1. Configuration of L-shape three-antenna InISAR imaging system

Denoting that the radar transmits Linear Frequency Modulation (LFM) signal with the carrier frequency f_c, bandwidth *B*, pulse duration time T_p, pulse interval T_r, dwell time T_1, and the scattering intensity σ_k for the *k*th scatterer. And *c* means the light velocity, the wavelength is λ, the chirp rate is γ. All the three radars generally use the same reference distance R_{refA} to dechirp. Denoting $R_{\Delta Ak}=R_{Ak}-R_{refA}$, $R_{\Delta Bk}=R_{Bk}-R_{refA}$, $R_{\Delta Ck}=R_{Ck}-R_{refA}$ and $R_{refA}=R_{AO}$.

InISAR imaging technology is a combination of high-resolution ISAR imaging and interferometric technique. Therefore, high-resolution ISAR image is the precondition of the InISAR 3D imaging. According to the existing motion compensation and pulse compression methods, high-resolution ISAR images can be obtained. The high-resolution ISAR imaging results obtained by the three radars can be written as:

$$S_A(f, f_m)=\sum \sigma_k T_p T_1 \sin c\left[T_p\left(f_i-\frac{2\gamma}{c}R_{\Delta Ak}\right)\right]\sin c\left[T_1\left(f_m-\frac{2V_{Ak}}{\lambda}\right)\right]\exp\left(-j\frac{4\pi R_{\Delta Ak0}}{\lambda}\right) \quad (1)$$

$$S_B(f, f_m)=\sum \sigma_k T_p T_1 \sin c\left[T_p\left(f_i-\frac{\gamma}{c}(R_{\Delta Ak}+R_{\Delta Bk})\right)\right]\sin c\left[T_1\left(f_m-\frac{(V_{Ak}+V_{Bk})}{\lambda}\right)\right]\exp\left(-j\frac{2\pi(R_{\Delta Ak0}+R_{\Delta Bk0})}{\lambda}\right) \quad (2)$$

$$S_C(f, f_m)=\sum \sigma_k T_p T_1 \sin c\left[T_p\left(f_i-\frac{\gamma}{c}(R_{\Delta Ak}+R_{\Delta Ck})\right)\right]\sin c\left[T_1\left(f_m-\frac{(V_{Ak}+V_{Ck})}{\lambda}\right)\right]\exp\left(-j\frac{2\pi(R_{\Delta Ak0}+R_{\Delta Ck0})}{\lambda}\right) \quad (3)$$

Where *f* is the frequency relative to fast-time, f_m is the Doppler frequency relative to slow-time.

From (1) and (2), the mismatch for the *k*th scatterer between ISAR images $S_A(f, f_m)$ and $S_B(f, f_m)$ is:

$$\Delta f=\frac{\gamma}{c}(R_{\Delta Ak0}-R_{\Delta Bk0})=\frac{\gamma}{c}(R_{\Delta Ak}-R_{\Delta Bk})\big|_{t_m=0}=\frac{\gamma}{c}(R_{Ak}-R_{Bk})\big|_{t_m=0} \quad (4)$$

$$\Delta f_m=\frac{V_{Ak}-V_{Bk}}{\lambda}=\frac{(R_{Ak}-R_{Bk})\big|_{t_m=T_1}-(R_{Ak}-R_{Bk})\big|_{t_m=0}}{\lambda T_1} \quad (5)$$

After ISAR image registration, interferometric technique is introduced to obtain the 3D structure of the target. The relationship between the interferometric phase difference and the coordinates are:

$$\Delta\varphi_{AB}=-\varphi_A+\varphi_B=\frac{2\pi}{\lambda}(R_{\Delta Ak0}-R_{\Delta Bk0})=\frac{2\pi}{\lambda}\frac{2L(X_0+x_k)-L^2}{R_{Ak}+R_{Bk}} \quad (6)$$

$$\Delta\varphi_{AC}=-\varphi_A+\varphi_C=\frac{2\pi}{\lambda}(R_{\Delta Ak0}-R_{\Delta Ck0})=\frac{2\pi}{\lambda}\frac{2L(Y_0+z_k)-L^2}{R_{Ak}+R_{Bk}} \quad (7)$$

3 The proposed ISAR image registration method

3.1 Estimation of wave path difference

From (4) and (5), it can be seen that if the radars B and C use the same reference distance as R_{AO}, which is the exact distance from the target to radar A, the mismatch between ISAR images is serious. However, if the reference distances of radar B and radar C were manipulated to R_{BO} and R_{CO} respectively, the mismatch would be alleviated effectively. Namely, $R'_{\Delta Bk}=R_{Bk}-R_{BO}$, $R'_{\Delta Ck}=R_{Ck}-R_{CO}$. Then, the mismatch in range and cross-range can be written as follow:

$$\begin{aligned}\Delta f' &= \frac{\gamma}{c}\left(R_{\Delta Ak0}-R'_{\Delta Bk0}\right)=\frac{\gamma}{c}\left[\left(R_{Ak}-R_{Bk}\right)-\left(R_{AO}-R_{BO}\right)\right]\big|_{t=0} \\ &< \frac{\gamma}{c}\left[\left(R_{Ak}-R_{Bk}\right)-\left(R_{AO}-R_{AO}\right)\right]\big|_{t_m=0}=\frac{\gamma}{c}\left[R_{Ak}-R_{Bk}\right]\big|_{t_m=0}\end{aligned} \quad (8)$$

$$\begin{aligned}\Delta f'_m &= \frac{1}{\lambda}\left[\left(R_{\Delta Ak}-R'_{\Delta Bk}\right)\big|_{t_m=T_1}-\left(R_{\Delta Ak}-R'_{\Delta Bk}\right)\big|_{t_m=0}\right] \\ &= \frac{1}{\lambda}\left\{\left[\left(R_{Ak}-R_{Bk}\right)-\left(R_{AO}-R_{BO}\right)\right]\big|_{t_m=T_1}-\left[\left(R_{Ak}-R_{Bk}\right)-\left(R_{AO}-R_{BO}\right)\right]\big|_{t_m=0}\right\} \\ &< \frac{1}{\lambda}\left\{\left[\left(R_{Ak}-R_{Bk}\right)-\left(R_{AO}-R_{AO}\right)\right]\big|_{t_m=T_1}-\left[\left(R_{Ak}-R_{Bk}\right)-\left(R_{AO}-R_{AO}\right)\right]\big|_{t_m=0}\right\} \\ &= \frac{1}{\lambda}\left[\left(R_{\Delta Ak}-R_{\Delta Bk}\right)\big|_{t_m=T_1}-\left(R_{\Delta Ak}-R_{\Delta Bk}\right)\big|_{t_m=0}\right]\end{aligned} \quad (9)$$

Consequently, the wave path difference that radar B and C needs compensating is:

$$\Delta R_m^B=R_{AO}-R_{BO} \quad (10)$$

$$\Delta R_m^C=R_{AO}-R_{CO} \quad (11)$$

Furthermore, the compensation phase corresponding to the abovementioned wave path difference in (10) and (11) should be constructed to compensate the received echoes of radar B and C, which are as follow:

$$Pha_m^B=\exp\left\{-j2\pi\gamma\hat{t}\Delta R_m^B/c\right\}\exp\left\{-j2\pi\Delta R_m^B/\lambda\right\} \quad (12)$$

$$Pha_m^C=\exp\left\{-j2\pi\gamma\hat{t}\Delta R_m^C/c\right\}\exp\left\{-j2\pi\Delta R_m^C/\lambda\right\} \quad (13)$$

Based on the above analysis, the main reason for the mismatch of the ISAR images is the wave path difference from the scatterer to different radar. Therefore, the main purpose of this section is to estimate and compensate the

wave path difference. And a wave path difference estimation method based on angle motion parameter estimation is proposed.

According to the derivation in Section III in [9], the difference between $R_{AO}(t_m)$ and $R_{BO}(t_m)$ can be modelled as:

$$\Delta R_m^B = R_{AO}(t_m) - R_{BO}(t_m) = L\sin\left(\theta(t_m)\text{-}\theta(t_0)\right) \approx L \bullet w^{AB} t_m \quad (14)$$

Similarly, the reference distance difference between radar A and radar C is $\Delta R_m^C \approx L \bullet w^{AC} t_m$.

Where the rotational angular velocities w^{AB} and w^{AC} are the projections of real rotational angular velocity w in XOY plane and ZOY plane.

Consequently, the ISAR image registration problem is transformed from the problem of wave path difference estimation to the problem of target rotational angle estimation.

3.2 Estimation of rotational angle based on chirp Fourier transform.

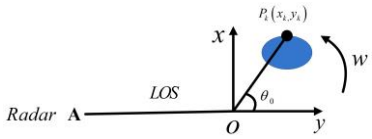

Figure 2. Turntable model of ISAR imaging

Based on the turntable model in Figure 2, for the targets with uniform rotational angular velocity relative to radar A, the distance from scatterer P_k to radar A is:

$$\begin{aligned} R_{Ak} &= R_{AO} + R_{\Delta Ak} = R_{AO} + R_{Ok}\cos(\theta_0 + wt_m) \\ &= R_{AO} + \sqrt{x_k^2 + y_k^2}\left(\cos\theta_0 \cos wt_m - \sin\theta_0 \sin wt_m\right) \\ &= R_{AO} + y_k \cos wt_m - x_k \sin wt_m \end{aligned} \quad (15)$$

Then, after eliminating remaining video phase and envelope skew, the range profile for radar A is:

$$S_A(f, t_m) = \sum \sigma_k T_p \sin c\left(T_p\left(f + \frac{2\gamma}{c} R_{\Delta Ak}\right)\right)\exp\left(-j\frac{4\pi}{\lambda} R_{\Delta Ak}\right) rect\left(\frac{t_m}{T_1}\right) \quad (16)$$

Where $R_{\Delta Ak} = y_k \cos wt_m - x_k \sin wt_m$, then the Doppler phase in (16) is:

$$Phase_{di} = \exp\left\{-j\frac{4\pi\left(y_k \cos wt_m - x_k \sin wt_m\right)}{\lambda}\right\} \quad (17)$$

Consequently, when the rotational angle is small, the Doppler frequency can be obtained as follow:

$$f_{dci} = \frac{1}{2\pi}\frac{dPhase_{di}}{dt_m} = -\frac{2w}{\lambda}\left(y_k \sin wt_m + x_k\right) \approx -\frac{2w}{\lambda}x_k - \frac{2y_k w^2}{\lambda}t_m \quad (18)$$

From (18), the signal in the slow-time domain is LFM signal, and the chirp rate is:

$$k = -\frac{2y_k w^2}{\lambda} \quad (19)$$

Equation (19) indicates that rotational angular velocity w is the dependent variable of the chirp rate k, given the wave length λ and the scatterer coordinate y_k. In other words, it should be noted that the estimation of the rotational angular velocity is equivalent to the estimation of the chirp rate in the slow-time domain. Hence the chirp Fourier transform is introduced as an efficient tool to estimate the chirp rate k. The chirp Fourier transform of range profile is defined as:

$$F(f, \gamma) = \int S_A(f, t_m)\exp\left[j2\pi \bullet \frac{1}{2}\gamma t_m^{\,2}\right] dt_m \quad (20)$$

Where the scope of the compensated chirp rate γ is:

$$\gamma = \frac{2y_k w}{\lambda} \in \left\{\frac{2y_k w_{\min}}{\lambda}, \frac{2y_k w_{\max}}{\lambda}\right\} \quad (21)$$

For each chirp rate γ in the scope, the entropy corresponding to its chirp Fourier transform result $F(f, \gamma)$ is calculated. Then, the chirp rate parameter γ, whose chirp Fourier transform result has the minimum entropy, is selected as the parameter estimation result of chirp rate of the echo Doppler frequency. The definition of entropy is as written in Section IV in [10]. Furthermore, to obtain a more robust chirp rate parameter estimation result, the range profiles of the range cells around the strong scattering range cell are selected as the range profile block (the change of the chirp rate is little), which is used to estimate the chirp rate. After obtaining the chirp rate of each range profile block, according to the linear relationship between the chirp rate and the distance y_k of the scatterer, as is shown in (19), the least squares fit method is used to fit the chirp rates obtained from the multiple range profile blocks. And the relationship between slope k of the fitted line and the rotational angular velocity is:

$$w = \sqrt{|k|\lambda / 2} \quad (22)$$

From the above, the flowchart of the whole target rotational angular velocity estimation algorithm is shown in Figure 3.

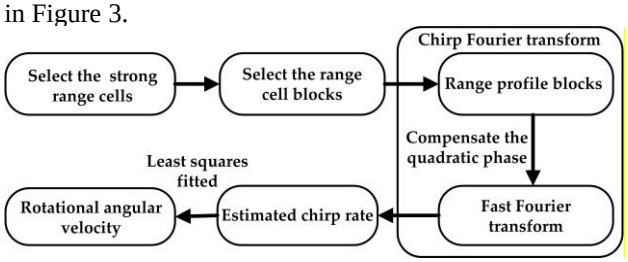

Figure 3. Flowchart of the rotational angular velocity estimation algorithm

3.3 Image registration based on wave path difference compensation.

After the rotational angular velocity estimation, the compensation phase is constructed to eliminate the effect of wave path difference on image mismatch. Hence, the concrete procedure of InISAR 3D imaging is as follows:

1) Estimate the rotational angular velocity based on chirp Fourier transform;
2) Calculate the wave path difference between centroid of target and different radars: $L \bullet w^{AB} t_m$ and $L \bullet w^{AC} t_m$;
3) Implement wave path difference compensation for the received echoes of radar B and radar C;
4) Yield the ISAR images of target without mismatch;
5) Implement interferometric between registered ISAR images to form the 3D structure of the target.

4 Experiment

In this section, the ISAR image registration method based on wave path difference compensation is validated and compared with the method based on correlation coefficient. The configuration of InISAR imaging is shown in Figure 1, the baseline L is 10m. The parameters of the radar system and the target are shown in Table 1.

Table.1 The parameters of radar and target

Radar	Carrier frequency f_c	10GHz
	Pulse duration T_P	0.1ms
	Bandwidth B	1GHz
	Pulse Repeat Frequency	100Hz
	Pulse number	500
Target	Scatterer number	8
	Rotational angular velocity	0.0112rad/s

4.1 Result of the image registration based on wave path difference compensation.

The estimation results of the echo Doppler chirp rate γ are shown in Figure 4, in which the blue dotted line shows the estimated results of the chirp Fourier transform for each range profile block, and the red line is the least squares fitted result. Then, the estimation result of the rotational angular velocity w is: $w = \sqrt{-\lambda k / 2} = 0.0111$.

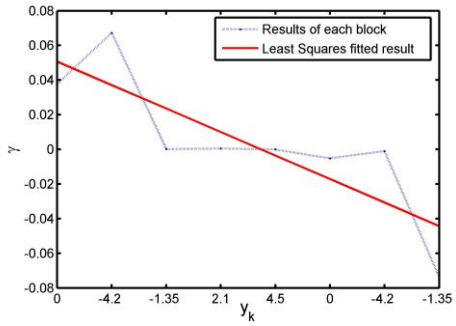

Figure 4. Estimation results of the Doppler chirp rate

As is shown in Figure 5, the range profiles of three radars are of high similarity, which indicates that the mismatch along range direction is eliminated. After pulse compression along cross-range direction, the ISAR images of the target are obtained. For convenience sake, the positions of the strong scatterers in the ISAR images can be extracted in Table 2. The first number in parentheses is scatterer position along cross-range cell, and the second one is the position along range cell. As can be seen from the Table 2, the positions of the strong scatterers in the three ISAR images of three different radars are identical, namely, the mismatch between the ISAR images is eliminated. In other words, image registration is accomplished.

Since the ISAR image registration is the intermedium step of the interferometric ISAR imaging process, hence the ultimate InISAR 3D imaging results should be used to measure the performance of the proposed method. According to Section 3.3, the x and z coordinates of the scatterer can be obtained. And the y coordinate is relative to the distance of scatterer along range direction. The 3D imaging result is shown in Figure 6, the blue dots indicate the true structure of the target, and the red circles indicate the 3D imaging result. The average coordinates (x, y, z) difference between the red circle and the relative blue dot is 0.3034. It is visible that the proposed method can effectively implement ISAR image registration of an L-shaped three-antenna InISAR imaging system. More importantly, InISAR 3D imaging works well.

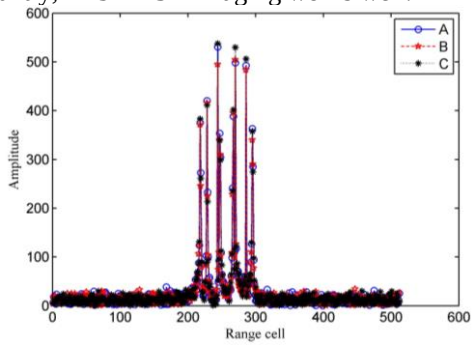

Figure 5. Range profiles without mismatch

Table 2. The location of scatterer in ISAR images

Number	A	B	C
1	(247,218)	(247,218)	(247,218)
2	(279,229)	(279,229)	(279,229)
3	(229,243)	(229,243)	(229,243)
4	(260,248)	(260,248)	(260,248)
5	(253,267)	(253,267)	(253,267)
6	(242,269)	(242,269)	(242,269)
7	(256,286)	(256,286)	(256,286)
8	(244,295)	(244,295)	(244,295)

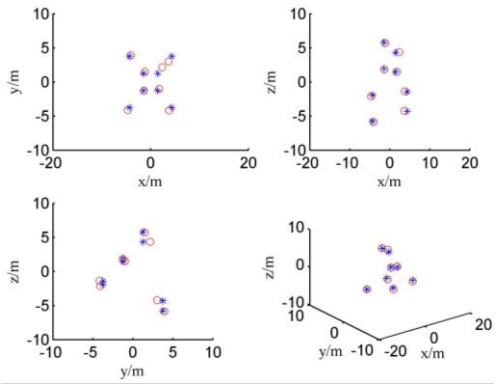

Figure 6. InISAR imaging result through the proposed method

4.2 The experiment results of the image registration based on correlation coefficient.

As is shown in Figure 7, the correlation coefficient between image A and image B and image C are calculated. The eclipse time of the correlation between image A and image B is 15916s, and that between image A and image C is 15740s. The simulation was conducted on MATLAB software on computer configured with an Intel(R) Core™ i7 7700 CPU @ 3.6 GHz and 16 GB RAM. From the results in Figure 7, the optimal shift

amount of the image B is 0.8 pixels along range direction and 18.3 pixels along cross-range direction, and that of the image C is 0.7 pixels along range direction and 10.8 pixels along cross-range direction. Image B and image C is shifted, respectively, based on the optimal shift amount of B and C. Additionally, the positions of strong scatterers are extracted in Table 3. It is obvious that there is still mismatch between ISAR images of different radars. Therefore, the registration accuracy of the registration method based on the correlation coefficient is poor. And, finally, InISAR 3D imaging is inefficient with correlation-based method, as shown in Figure 8. The average coordinates (x, y, z) difference between the red circle and the relative blue dot is 45.8529.

In conclusion, the method based on wave path difference compensation can effectively complete the ISAR image registration, and the InISAR imaging quality of it is better than that of the correlation-based method.

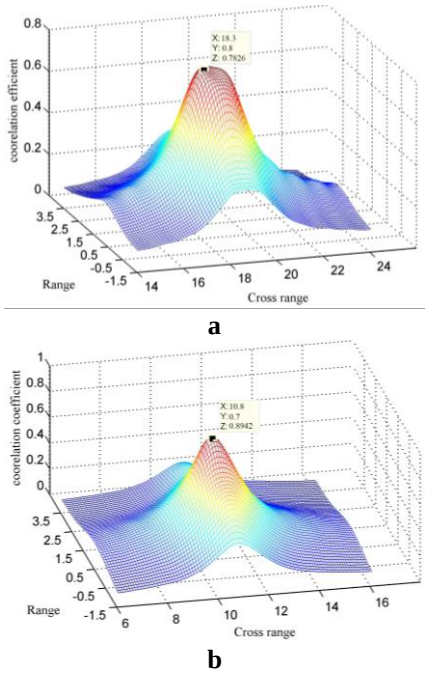

Figure 7. Distribution of correlation coefficients during registration;
(a) Radar B (range 0.8, cross-range 18.3, eclipse time:15916s),
(b) Radar C (range 0.7, cross-range 10.8, eclipse time:15740s).

Table 3. The mismatched scatterer in ISAR image

Number	A	B	C
1	(247,218)	(246,218)	(247,218)
2	(279,229)	(278,229)	(278,230)
3	(229,243)	(229,243)	(229,243)
4	(260,248)	(260,247)	(260,248)
5	(253,267)	(252,266)	(253,267)
6	(242,269)	(242,269)	(241,270)
7	(256,286)	(256,286)	(256,286)
8	(244,295)	(243,295)	(244,295)

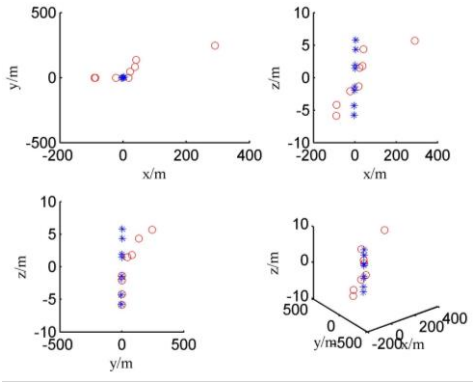

Figure 8. InISAR imaging result through the method based on correlation efficient

5 Conclusion

In this paper, a novel ISAR image registration method based on wave path difference compensation is proposed. The proposed method eliminates the wave path difference between the scatterer and different radars by the wave path difference phase compensation in echo field, and achieves ISAR image registration. In comparison to the ISAR image registration method based on correlation coefficient, the proposed method is more precise and more efficient significantly. In brief, the proposed ISAR image registration method based on wave path difference compensation has advantages in precision and computing efficiency, compared with precedent methods.

References

1. Wang, G., Xia, X., Chen Victor, C.: Three-dimensional ISAR imaging of maneuvering targets using three receivers, IEEE Trans. Image Process., 10, (3), pp. 436–447, 2001.
2. Tian B, Zou J, Xu S, et al. Squint model interferometric ISAR imaging based on respective reference range selection and squint iteration improvement[J]. Radar Sonar & Navigation Iet, 9(9):1366-1375, 2015.
3. Chen C C, Andrews H C. Target-Motion-Induced Radar Imaging[J]. Aerospace & Electronic Systems IEEE Transactions on, AES-16(1):2-14, 1980.
4. Martorella M, Stagliano D, Salvetti F, et al. 3D interferometric ISAR imaging of noncooperative targets[J]. Aerospace & Electronic Systems IEEE Transactions on, 50(4):3102-3114, 2014.
5. Tian B, Li N, Liu Y, et al. A novel image registration method for InISAR imaging system[C] Millimetre Wave and Terahertz Sensors and Technology VII. International Society for Optics and Photonics, 2014.
6. Stagliano D, Lischi S, Massini R, et al. Soft 3D-ISAR image reconstruction using a dual interferometric radar [C] Radar Conference. IEEE:0572-0576, 2015.
7. Nasirian M, Bastani M H. A Novel Model for Three-Dimensional Imaging Using Interferometric ISAR in Any Curved Target Flight Path[J]. IEEE Transactions on Geoscience & Remote Sensing, 52(6):3236-3245, 2014.

8. Wang Q, Jishuang Q U, Huang H, et al. A Method Based on Integrating Real and Complex Correlation Function for InSAR Image Coregistration[J]. Acta Geodaetica Et Cartographica Sinica, 2012.
9. Zhang Q, Yeo T S, Du G, et al. Estimation of three-dimensional motion parameters in interferometric ISAR imaging[J]. Geoscience & Remote Sensing IEEE Transactions on, 42(2):292-300, 2004.
10. Wu W, Hu P, Xu S, et al. Image registration for InISAR based on joint translational motion compensation[J]. Iet Radar Sonar & Navigation, 11(10):1597-1603, 2017.